ISSN 1028-334X, Doklady Earth Sciences, 2007, Vol. 412, No. 1, pp. 94–96. © Pleiades Publishing, Ltd., 2007.
Original Russian Text © S.A. Sadykov, V.A. Popov, V.N. Anfilogov, T.P. Nishanbaev, 2007, published in Doklady Akademii Nauk, 2007, Vol. 412, No. 2, pp. 250–252.

GEOCHEMISTRY

Zonal Distribution of Carbon Isotopes in Supergene Calcite Crystals from the Dal'negorsk Deposit, Primor'e Region

S. A. Sadykov, V. A. Popov, Corresponding Member of the RAS
V. N. Anfilogov, and T. P. Nishanbaev

Received August 18, 2006

DOI: 10.1134/S1028334X07010217

Study of the geochemistry of stable isotopes can efficiently solve issues of the genetic mineralogy only if we can define the sources of matter involved in mineral formation. The present paper reports original data on the distribution of carbon isotopes in two types of supergene calcite. Calcite of type 1 was sampled from stalactites in karst cavities in Triassic limestone blocks. Calcite of type 2 is a product of the reaction of wollastonite with CO_2-rich groundwaters. The isotopic composition of calcite was determined with a Delta+ Advantage (Thermo Finnigan) mass spectrometer. The accuracy of $\delta^{13}C$ determination was 0.07‰ PDB. Material for the analysis was taken with a diamond drill 3.5 mm in diameter.

Calcite 1 was precipitated from $CaCO_3$-rich groundwaters. Carbon entered this mineral as carbonate ions from limestones and CO_2-rich meteoric waters. Therefore, summer layers of stalactite should be enriched in atmospheric carbon, whereas winter layers should be enriched in limestone. Figure 1 shows the transverse section of a stalactite specimen with a zonal growth pattern. The specimen (13 × 10 cm in size) was taken from a cave in limestones near Dal'negorsk. The specimen clearly shows zones with different colors. Figure 2 presents a bar chart of the distribution of carbon isotopes in different zones. Samples for the analysis were taken with an average spacing of 1 cm. Numerations 2 and 3 designate early growth zones of carbonates. The maximum discrepancy in the isotopic composition between these zones is 4.15‰ PDB. Since the sample dimension is significantly smaller than the growth zone width, the maximum $\delta^{13}C$ value can be underestimated and the minimum value can be overestimated. Nevertheless, the distribution pattern shows that the $\delta^{13}C$ value changed periodically in the course of stalactite growth. The minimum value (–11.49‰ PDB) should be assigned to the $\delta^{13}C$ content in limestones; the maximum value (–7.34‰ PDB), to the $\delta^{13}C$ content in waters enriched with atmospheric carbon dioxide.

Calcite 2 is a tabular monocrystal (hexagonal prism), 2.3 × 3.0 cm in size and ~2 mm in thickness (Fig. 3), representing a combination of pinacoid {0001}, prism {10–10}, and tiny faces of scalenohedron. The crystal shows distinct zonality. The specimen was separated into the following four zones: (zone I) central dull part (seed); (zone II) transparent zone around the seed; (III) opaque white zone; and (zone IV) transparent peripheral zone. The crystal was preliminarily treated in 10%-HCl for 10 min to clean the surface and reveal the morphology of growth zones.

At high magnification, transparent zones II and IV show numerous thin zones parallel to faces of the prism {10–10}. The minimum thickness of such zones is 10 μm.

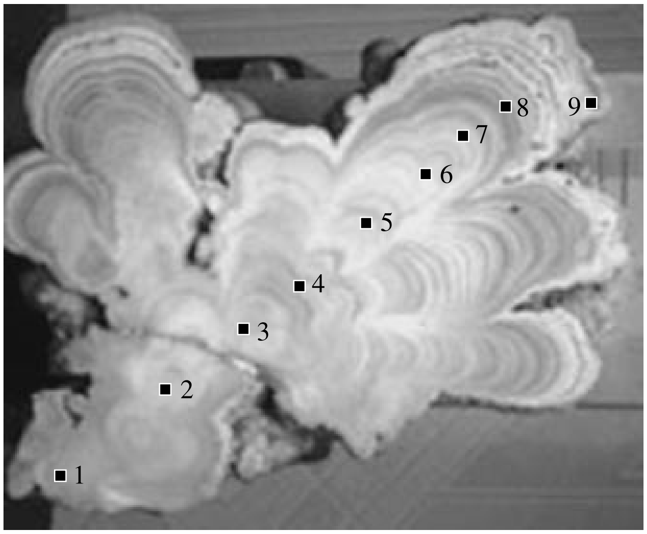

Fig. 1. Specimen of zonal carbonate (flowstone). (■) Sampling sites and sample numbers.

Institute of Mineralogy, Ural Division,
Russian Academy of Sciences, Miass, Chelyabinsk oblast,
456317 Russia; e-mail: sadykov@ilmeny.ac.ru

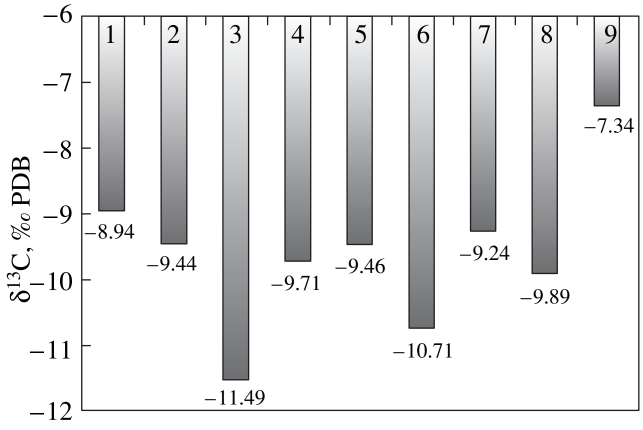

Fig. 2. Bar charts of δ^{13}C values in the flowstone sample. Sample numbers are as in Fig. 1.

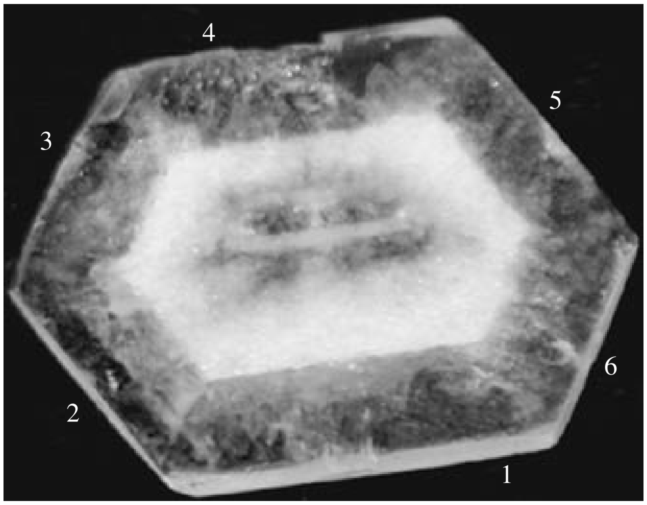

Fig. 3. Calcite specimen from the Bor deposit (Tetyukhe, Primor'e region). Numerals designate faces where samples were taken for the measurement of ^{13}C/^{12}C values.

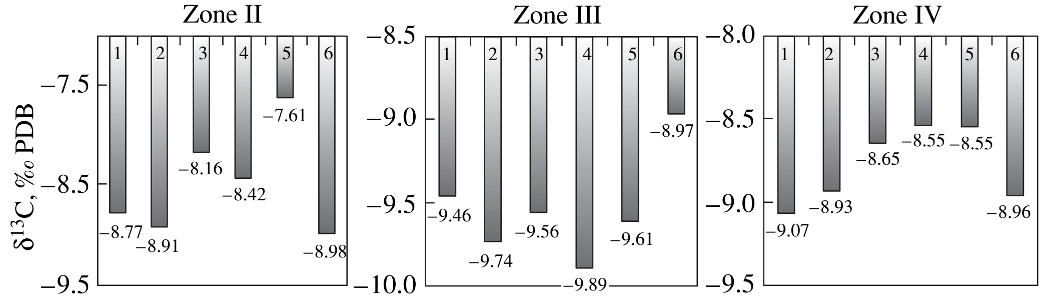

Fig. 4. Bar charts of δ^{13}C values in the calcite crystal in zones II–IV. Numeration of faces is as in Fig. 3.

The transverse section of zone I reveals a great number of cracks related to growth stress. Under the binocular microscope, one can see that the cracks inherit surfaces of translation apices {10–11}; i.e., the pinacoid {0001} underwent drastic degeneration into the cleavage rhombohedron {10–11} in such sectors. Zone I reveals numerous tiny pyramids that represent cleavage rhombohedra {10–11} restricted by the pinacoid. The tiny pyramids (hereafter, rhombohedra) are oriented strictly relative to each other, while faces of different rhombohedra are parallel. The base of the rhombohedra is parallel to the pinacoid {0001}, while lateral faces are parallel to faces of the outer prism {10–10}. A similar pattern is observed in zone III.

The central part of the crystal includes a dull seed extended along axis L_2 of calcite. The transparent wide zone in the seed shows a combination of pinacoid with different faces. The combination of pinacoid with faces of rhombohedron and scalenohedron produces trigonal growth patterns. Ultimately, we observe the following succession of growth zones. The crystal core includes a prismatic seed with faces {0001} and {10–11}. This zone is overgrown with the remaining portion of the crystal. In opaque zones, one can observe a drastic change of shape from {0001} to {10–11}. Transparent sectors are related to a slower zonal growth of the crystal. The zonality of the crystal is also supported by its morphological features. One can observe the following successive episodes of crystal growth:

(1) growth with drastic change of shape from {0001} to {10–10};

(2) zonal overgrowth along faces {0001} and {10–11};

(3) a new episode of overgrowth with drastic change of shape from {0001} to {10–10}; and

(4) zonal growth of faces {10–10}.

We took calcite samples from the pinacoid surface along sectors corresponding to different faces of the prism for each of the four zones. Since the crystal has a very fine zonal structure, materials from different growth layers inside a single zone could enter the sample taken for analysis. Therefore, variations in the δ^{13}C value reflect only the trend of periodic fluctuations of this parameter in the course of crystal growth. Figure 4 presents bar charts of $\delta^{13}C$ distribution in zones II–IV and different faces.

Supergene calcite crystals in the Dal'negorsk deposit formed together with quartz crystals in the course of the reaction of wollastonite with groundwaters enriched in carbonate ions:

$$CaSiO_3 + CO_2 = CaCO_3 + SiO_2.$$

This reaction is fostered by the following situation. At low temperatures, the free energy of calcite formation becomes higher than the ΔG value for wollastonite. As in the case of the formation of stalactites, the decomposition of wollastonite took place under the influence of two sources of carbon (atmospheric carbon dioxide and older calcite that was present in wollastonite–datolite ores). The atmospheric carbon dioxide has a typical $\delta^{13}C$ value of –7‰ PDB [1]. The minimum $\delta^{13}C$ value (–9.89‰ PDB) recorded in the calcite reflects the contribution of the older calcite, which was generated in the course of the dissolution of limestone. This value is much lower than that in the stalactite. Hence, the second source played a subordinate role during the growth of the crystal relative to the growth of the stalactite.

REFERENCES

1. G. Faure, *Principles of Isotope Geology* (Wiley, New York, 1986; Mir, Moscow, 1989).